



THE UNIVERSITY *of* EDINBURGH

Edinburgh Research Explorer

APOE ϵ 4 exacerbates age-dependent deficits in cortical microstructure.

Citation for published version:

Mak, E, Dounavi, M-E, Operto, G, Ziukelis, ET, Jones, PS, Low, A, Swann, P, Newton, C, Muniz Terrera, G, Malhotra, P, Koychev, I, Falcon, C, Mackay, C, Lawlor, B, Naci, L, Wells, K, Ritchie, C, Ritchie, K, Su, L, Gispert, JD, O'Brien, JT & PREVENT-Dementia and ALFA studies 2024, 'APOE ϵ 4 exacerbates age-dependent deficits in cortical microstructure.', *Brain Communications*, vol. 6, no. 1, pp. fcad351. <https://doi.org/10.1093/braincomms/fcad351>

Digital Object Identifier (DOI):

[10.1093/braincomms/fcad351](https://doi.org/10.1093/braincomms/fcad351)

Link:

[Link to publication record in Edinburgh Research Explorer](#)

Document Version:

Publisher's PDF, also known as Version of record

Published In:

Brain Communications

General rights

Copyright for the publications made accessible via the Edinburgh Research Explorer is retained by the author(s) and / or other copyright owners and it is a condition of accessing these publications that users recognise and abide by the legal requirements associated with these rights.










Take down policy

The University of Edinburgh has made every reasonable effort to ensure that Edinburgh Research Explorer content complies with UK legislation. If you believe that the public display of this file breaches copyright please contact openaccess@ed.ac.uk providing details, and we will remove access to the work immediately and investigate your claim.



BRAIN COMMUNICATIONS

APOE ϵ 4 exacerbates age-dependent deficits in cortical microstructure

 **Elijah Mak**,¹  **Maria-Eleni Dounavi**,¹ **Grégory Operto**,² **Elina T. Ziukelis**,¹ **Peter Simon Jones**,³  **Audrey Low**,¹ **Peter Swann**,¹  **Coco Newton**,¹ **Graciela Muniz Terrera**,⁴  **Paresh Malhotra**,⁵  **Ivan Koychev**,⁶ **Carles Falcon**,^{2,7,8}  **Clare Mackay**,⁶ **Brian Lawlor**,⁹ **Lorina Naci**,⁹ **Katie Wells**,⁴ **Craig Ritchie**,⁴ **Karen Ritchie**,^{10,11} **Li Su**,¹  **Juan Domingo Gispert**^{2,7,8} and  **John T. O'Brien**¹; on behalf of the PREVENT-Dementia and ALFA studies and TRIBEKA Consortium

The apolipoprotein E ϵ 4 allele is the primary genetic risk factor for the sporadic type of Alzheimer's disease. However, the mechanisms by which apolipoprotein E ϵ 4 are associated with neurodegeneration are still poorly understood. We applied the Neurite Orientation Dispersion Model to characterize the effects of apolipoprotein ϵ 4 and its interactions with age and education on cortical microstructure in cognitively normal individuals. Data from 1954 participants were included from the PREVENT-Dementia and ALFA (Alzheimer and Families) studies (mean age = 57, 1197 non-carriers and 757 apolipoprotein E ϵ 4 carriers). Structural MRI datasets were processed with FreeSurfer v7.2. The Microstructure Diffusion Toolbox was used to derive Orientation Dispersion Index maps from diffusion MRI datasets. Primary analyses were focused on (i) the main effects of apolipoprotein E ϵ 4, and (ii) the interactions of apolipoprotein E ϵ 4 with age and education on lobar and vertex-wise Orientation Dispersion Index and implemented using Permutation Analysis of Linear Models. There were apolipoprotein E ϵ 4 \times age interactions in the temporo-parietal and frontal lobes, indicating steeper age-dependent Orientation Dispersion Index changes in apolipoprotein E ϵ 4 carriers. Steeper age-related Orientation Dispersion Index declines were observed among apolipoprotein E ϵ 4 carriers with lower years of education. We demonstrated that apolipoprotein E ϵ 4 worsened age-related Orientation Dispersion Index decreases in brain regions typically associated with atrophy patterns of Alzheimer's disease. This finding also suggests that apolipoprotein E ϵ 4 may hasten the onset age of dementia by accelerating age-dependent reductions in cortical Orientation Dispersion Index.

1 Department of Psychiatry, School of Clinical Medicine, University of Cambridge, Cambridge CB2 0QQ, UK

2 BarcelonaBeta Brain Research Center, Pasqual Maragall Foundation, Barcelona 08005, Spain

3 Department of Clinical Neurosciences, University of Cambridge, Cambridge CB2 0SZ, UK

4 Centre for Dementia Prevention, University of Edinburgh, Edinburgh EH4 2XU, UK

5 Department of Brain Sciences, Imperial College, London W12 0NN, UK

6 Department of Psychiatry, Oxford University, Oxford OX3 7JX, UK

7 IMIM (Hospital del Mar Medical Research Institute), Barcelona 08003, Spain

8 Centro de Investigación Biomédica en Red de Bioingeniería, Biomateriales y Nanomedicina (CIBER-BBN), Madrid 28029, Spain

9 Institute of Neuroscience, Trinity College Dublin, University of Dublin, Dublin D02 PX31, Ireland

10 Institut National de la Santé et de la Recherche Médicale, U1061 Neuropsychiatrie, Montpellier 34093, France

11 Faculty of Medicine, University of Montpellier, Montpellier 34093, France

Correspondence to: John T. O'Brien

Department of Psychiatry

University of Cambridge School of Clinical Medicine

Level E4 Cambridge Biomedical Campus

Received May 30, 2023. Revised October 20, 2023. Accepted February 09, 2024. Advance access publication February 21, 2024

© The Author(s) 2024. Published by Oxford University Press on behalf of the Guarantors of Brain.

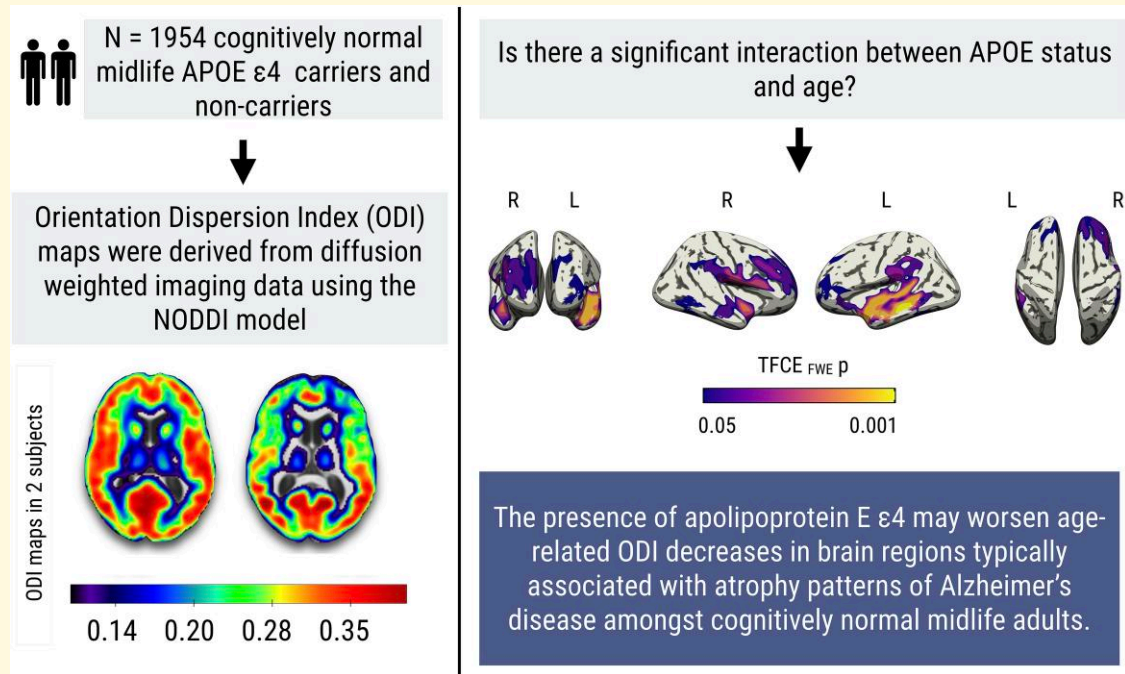
This is an Open Access article distributed under the terms of the Creative Commons Attribution License (<https://creativecommons.org/licenses/by/4.0/>), which permits unrestricted reuse, distribution, and reproduction in any medium, provided the original work is properly cited.

Cambridge CB2 0SP, UK
E-mail: john.obrien@medschl.cam.ac.uk

Correspondence may also be addressed to: Juan Domingo Gispert
Barcelonaβeta Brain Research Center
Pasqual Maragall Foundation, Barcelona 08005, Spain
E-mail: jdgispert@barcelonabeta.org

Keywords: NODDI; neurodegeneration; cognitive impairment; preclinical dementia

Graphical Abstract



Introduction

The *APOE* ϵ 4 allele is the strongest genetic risk factor for both sporadic early and late-onset Alzheimer's disease.^{1,2} A growing body of neuroimaging studies has delineated the imaging phenotypes of *APOE* ϵ 4 in cognitively normal individuals as a means to detect preclinical changes that may occur before cognitive impairment (for systematic reviews, see^{3,4}) Some notable findings in middle-aged *APOE* ϵ 4 carriers include (i) grey matter atrophy in typical Alzheimer's disease regions,⁵⁻⁷ (ii) diffusion tensor imaging (DTI) changes in white matter tracts,⁸ (iii) functional deficits in cerebral perfusion and glucose metabolism⁹⁻¹¹ as well as (iv) disruptions in both task-based functional MRI^{12,13} and intrinsic connectivity within resting-state networks.¹⁴

Nonetheless, definitive evidence for a *APOE* ϵ 4 'signature' remains elusive due to null results and inconsistent observations. In addition to methodological discrepancies, small *APOE* ϵ 4 effect sizes and sample variability across cohorts, contradictory results may also be attributed to the complex

midlife effects of the *APOE* ϵ 4 gene as well as its interactions with other pathological markers of Alzheimer's disease (i.e. amyloid and tau). The associations between *APOE* ϵ 4 and brain imaging changes and cognition in midlife adults may to some extent be modulated by sex and cognitive reserve.^{15,16} Similarly, a growing body of evidence suggests that the presence of *APOE* ϵ 4 may exacerbate the trajectory of age-related biomarker changes, with older *APOE* ϵ 4 homozygotes exhibiting an accelerated decline in white matter microstructural integrity,⁸ myelination (i.e. MRI T₁-weighted/T₂-weighted ratio),¹⁷ grey matter volumes and hippocampus shape.^{18,19}

It is also conceivable that the deleterious effects of *APOE* ϵ 4 are more pronounced at the cellular level of neurite morphology (i.e. dendritic arborization) and so would not be easily detected by macroscale analysis of standard MRI biomarkers. This notion is reinforced by histological evidence linking *APOE* ϵ 4 to several synaptic and neuritic abnormalities.²⁰ Thus, to the extent that neuritic abnormalities precede major cell death or brain atrophy, imaging markers of grey matter microstructure may reveal some of

the earliest effects related to APOE ϵ 4 genotype. To this end, the mean diffusivity (MD) parameter from DTI has been shown to be sensitive to dendritic alterations in the hippocampus,²¹ and its applications have expanded to include the analysis of hippocampal subfields and cortical grey matter in patients with autosomal dominant Alzheimer disease,²² mild cognitive impairment (MCI) and Alzheimer's disease.²³⁻²⁵ Collectively, these findings underscore the potential for diffusion MRI to characterize subtle cortical microstructural deficits. However, given the inherent differences in image resolution between typical DTI (2 mm) and T₁-MRI sequences (1 mm), the cortical MD signal could be sensitive to overestimation due to the spill-in of high MD values from unrestricted 'free water' diffusion in the CSF.²⁶

Recent advances in diffusion-weighted imaging have led to the development of biophysical models, expanding the application of diffusion imaging beyond white matter to grey matter microstructure.²⁷ One particularly promising technique for the quantification of neurite morphology at the level of axons and dendrites is neurite orientation dispersion and density imaging (NODDI), which features a three-compartment model to distinguish signal from intra-neurite, extra-neurite and CSF. The Orientation Dispersion Index (ODI) from NODDI reflects the complexity or dispersion in brain tissue. Histological correlations between ODI and post-mortem measures of orientation complexity suggest that these NODDI and ODI may be used to characterize *in vivo* dendritic branching.^{28,29} Previous studies have also demonstrated strong negative associations between age and ODI, in keeping with the expectation that dendritic arborization reduces with normal ageing.^{30,31} A recent study by our group demonstrated a close relationship between ODI and synaptic density in individuals with primary tauopathies, lending credence to the interpretation of ODI as a proxy of synaptic function.³²

Given that Alzheimer's disease pathology accumulates for years before irreversible and observable macrostructural atrophy,³³ establishing NODDI as a measure of microstructural abnormalities during the asymptomatic period will be essential for early identification, improving prognosis, accurate disease-staging, and treatment monitoring. Though NODDI has shown promise in studies of normal ageing,^{8,30} early-onset Alzheimer's disease,³⁴ and other tauopathies,³² there is currently insufficient data to draw conclusions about the influence of APOE ϵ 4 on grey matter NODDI measurements in cognitively normal mid-life adults. In this multi-site study, the NODDI model is applied to characterize the effects of APOE ϵ 4 and its interactions with age and education on cortical microstructural changes in cognitively normal individuals recruited from the PREVENT-Dementia³⁵ and ALFAprojects.³⁶ Both PREVENT-Dementia and ALFA are prospective observational cohort studies with the overarching goal of clarifying the pathophysiology and pathogenic factors occurring during the preclinical phase of Alzheimer's disease. The goals of this research were to (i) compare APOE ϵ 4

carriers and non-carriers on measures of ODI measured within the lobes and vertex-wise, (ii) evaluate the extent to which APOE ϵ 4 interacts with age and education to determine ODI, and (iii) investigate whether NODDI provides novel insights beyond that provided by conventional biomarkers such as cortical thickness.

Materials and methods

Study participants

The recruitment for ALFA subjects consisted of two steps. First, 2743 cognitively healthy volunteers aged between 45 and 76 years were enrolled in the ALFA. Exclusion criteria included performance exceeding the established cut-off for a number of cognitive tests and the presence of a psychiatric diagnosis. Second, after APOE ϵ 4 genotyping, all participants homozygous for the ϵ 4 allele as well as carriers of the ϵ 2 allele were invited to undergo MRI scanning along with APOE ϵ 4 heterozygotes and non-carriers, matched for age and sex. The ALFA+ study was approved by the Independent Ethics Committee 'Parc de Salut Mar', Barcelona. All participants signed the informed consent form that had also been approved by the Independent Ethics Committee 'Parc de Salut Mar', Barcelona; 701 participants were recruited in the PREVENT-Dementia study from 5 study sites: West London ($n=210$), Edinburgh ($n=223$), Cambridge ($n=100$), Oxford ($n=68$) and Dublin ($n=100$). The main entry criteria were age 40–59 and the absence of dementia or other neurological disorders. Approval for the study has been given by the NHS Research Ethics Committee London Camberwell St-Giles.

Neuroimaging

For ALFA, MRI scans were obtained with a 3T scanner (Ingenia CX, Philips, Amsterdam, Netherlands) and included a T₁-weighted Turbo Field Echo sequence (repetition time = 10 ms, echo time = 5 s, flip angle = 8 and voxel size = 0.75 mm³ isotropic) and a diffusion weighted imaging (DWI) protocol (repetition time = 9 ms, echo time = 90 ms, 8 b_0 volumes, 64 $b=1000$ s/mm² volumes and voxel size = 2.2 mm³ isotropic). For PREVENT, a T₁-weighted magnetization prepared rapid gradient echo scan was acquired (repetition time = 2.3 s, echo time = 2.98 ms, flip angle = 9, and voxel size = 1 mm³ isotropic) on 3T Siemens scanners: Prisma fit (Oxford), Prisma fit (Cambridge), Verio (West London) and Skyra (Dublin and Edinburgh). The DWI protocol in PREVENT was as follows: repetition time = 11 s 700 ms, echo time = 90 ms, 1 b_0 volumes, 64 $b=1000$ s/mm² volumes, flip angle = 90, and voxel size = 2 mm³ isotropic.

Preprocessing

Image preprocessing and vertex-wise analyses were performed on a dedicated cluster composed of CPU nodes [Cambridge Service for Data-Driven Discovery (CSD3):

2×Intel Xeon Skylake 6142 processors, 2.6 GHz 16-core, 192GiB RAM per node], and GPU servers for the GPU-optimized parts of the processing pipeline (NVIDIA Tesla K40/K80 GPUs).

Structural MRI

T_1 structural MRI datasets from ALFA and PREVENT were preprocessed using identical procedures. MRI scans were first corrected for intensity inhomogeneities with the Advanced Normalization Toolbox N4 algorithm.³⁷ Automated surface-based reconstruction of the T_1 -MRI datasets was performed using FreeSurfer v7.2 (<http://surfer.nmr.mgh.harvard.edu/>).³⁸ Visual inspections of the scans were performed by two authors (E.M. and E.T.Z) to ensure that there were no severe errors in the surface constructions (i.e. global misclassification of grey and white matters). Minor edits were made conservatively on datasets with white matter or pial surface errors when necessary (see [Supplementary Materials](#) for an example of topological correction). Estimates of cortical thickness were determined using FreeSurfer by computing the average distance between grey matter/white matter and grey matter/CSF surfaces at each vertex across the cortical mantle. These thickness measurements were then projected to the inflated surface of the rebuilt brain of each subject.

Diffusion MRI

Preprocessing

Diffusion datasets were visually inspected for optimal coverage and to ensure minimal eddy-current distortions. Subjects were excluded if there were excessive Echo Planar Imaging (EPI) distortions, poor image quality or insufficient field-of-view coverage. First, the *dwidenoise* tool from MRTRIX (<https://www.mrtrix.org>) was used to perform denoising on the raw 4D DWI volumes to improve signal-to-noise ratio.³⁹ Second, the *mrdegibbs* tool was used to apply Gibbs ringing correction to get rid of ringing artefacts. Subsequently, the DWI datasets were stripped of nonbrain tissue using the Brain Extraction Tool. To confirm the accuracy of the masks, a visual inspection was undertaken, and manual modifications were performed as needed. Eddy currents and head movements were corrected with *eddy_openmp* in FSL (Version 6.0.5). Quantitative identification of slices with signal loss was performed using the *-repol* option, and outlier volumes were replaced by non-parametric predictions using the Gaussian process.⁴⁰ The *b*-matrix was subsequently reoriented by applying the rotational part of the affine transformation used during eddy correction.⁴¹

Neurite orientation dispersion and density imaging

Following eddy-current correction, we applied the NODDI model²⁷ using the Microstructure Diffusion Toolbox⁴² to generate ODI whole-brain maps. The diffusion signal within each brain voxel is described by NODDI as a combination of

intracellular, extracellular and CSF components. The intracellular compartment is modelled as a set of sticks with restricted diffusion perpendicular to the orientation of the axonal bundles and unimpeded diffusion along them in order to capture neurite membranes and myelin sheaths. The extracellular compartment is assumed to encompass the region surrounding the neurites, which is made up of glial cells and somas. Isotropic diffusion is used to represent the CSF compartment. The ODI is a tortuosity measure computed as the neurite dispersion coefficient. Values closer to 0 indicate less dispersion or well-aligned neurites, but values closer to 1 indicate greater dispersion, which is often associated with increased dendritic branching or complexity in grey matter.²⁹ The original paper established the feasibility of modelling the ODI from single-shell diffusion measurements.²⁷ Furthermore, single-shell ODI studies have been demonstrated to reproduce group-level differences from multi-shell DWI data, particularly analyses were limited to the grey matter.⁴³ The neurite density (NDI) maps were excluded from all analyses since prior research found significant discrepancies between the NDI maps from multi- and single-shell DWIs.^{27,43}

Coregistration and estimation of lobar ODI

The *b*₀ volumes were coregistered with the T_1 -MRI using FreeSurfer's Boundary-Based Registration.⁴⁴ In order to warp the cortical lobar labels to native DWI space using the inverse transformation that was utilized to coregister the *b*₀ to the T_1 -MRI, we used the `mri annotation2label` command with the `'-lobesStrict'` flag, followed by `mri label2vol` and `mri vol2vol`. The average ODI values for the parietal, occipital, temporal, cingulate and insula lobes were generated using `'mri segstats'`. Given the inherent resolution differences between DWI and T_1 -MRI, the lobar methodology depends less on the perfect alignment of fine sulcal areas and provides a robust method for detecting *APOE* ϵ 4-related alterations in the presence of potential image-coregistration difficulties. Furthermore, it has been shown that lobe averaged values of imaging derived cortical thickness levels were comparable to the range of values as reported by von Economo's histological measurements.^{45,46}

Vertex-wise ODI surfaces

In addition, we performed a vertex-wise analysis to provide a more nuanced understanding of the correlations between *APOE* ϵ 4 and topological ODI changes. In order to accomplish this, the ODI intensities were sampled from the midpoint of the cortical ribbon (i.e. 50% of the cortical thickness along the surface normal to the grey matter/white matter surface) and projected to an inflated surface using the `mri vol2surf` function in FreeSurfer, before smoothing at 15-mm Gaussian kernel.

ComBat harmonization

To attenuate site-related effects of ODI, we used ComBat to lobar ODI and vertex-wise ODI datasets using R and custom MATLAB scripts, respectively.⁴⁷ Age, sex and *APOE* ϵ 4

status were specified as biological factors to retain the biological variability of the data, as demonstrated by the expected correlations with age (Supplementary Materials). The outcomes of the multi-site harmonization and the effects of ComBat on ODI are depicted in subject-specific box plots of lobar ODI, ordered by the site (Supplementary Materials). After using ComBat, site effects on ODI were no longer statistically significant.

Statistical analyses

All statistical analyses were performed in R version 4.2.0 (22 April 2022). Demographic variables and characteristics of the cohort were reported as mean (standard deviation, SD) or number (percentage), and differences between the APOE ε4 carriers and non-carriers were compared using ANOVA, Kruskal–Wallis, and χ^2 tests, where appropriate. Individuals with the ε2/ε4, ε3/ε4 and ε4/ε4 genotypes were classified as APOE ε4 carriers and compared against the non-carriers (ε2/ε2, ε2/ε3 and ε3/ε3 genotypes). Our primary analyses focused on the (i) main effects of APOE ε4, and the (ii) interactions of APOE ε4 with age on lobar and vertex-wise ODI. Non-parametric permutation models were computed using Permutation Analysis of Linear Models (PALM; <https://fsl.fmrib.ox.ac.uk/fsl/fslwiki/PALM>). In addition, the quadratic term of age was examined in order to model nonlinear changes. Thus, a significant main effect of APOE ε4 would imply group-level differences in ODI, whereas a significant interaction term would be consistent with a ‘accelerating’ effect of APOE ε4 on age-dependent ODI changes. The R package ‘emmeans’ was used to estimate marginal effects and to estimate the earliest age at which differences between APOE ε4 carriers and non-carriers could emerge. (iii) Non-parametric permutation models were used to assess three-way interactions between formal education years, age, and APOE ε4 on ODI to determine the potential role of cognitive reserve in moderating the effects of APOE ε4 on ODI changes. Statistical results were reported after correcting for multiple comparisons using family wise error (FWE). The TFCE method was used to adjust for multiple comparisons in all vertex-wise analyses.

Table 1 Sample characteristics of the study sample

Variable	Overall, N = 1954	ε4+, N = 757	ε4–, N = 1197	P-value ^a
Age				0.73
Mean (SD)	57.03 (7.26)	56.92 (7.31)	57.10 (7.23)	
Range	40.00, 77.08	40.00, 75.36	40.00, 77.08	
Sex, n (%)				0.44
Female	1221 (62%)	465 (61%)	756 (63%)	
Male	733 (38%)	292 (39%)	441 (37%)	
Education (years)				0.23
Mean (SD)	14.43 (3.78)	14.58 (3.86)	14.34 (3.73)	
Range	0.00, 38.00	6.00, 38.00	0.00, 27.00	

^aWilcoxon rank sum test; Pearson's Chi-squared test.
Abbreviation: APOE, Apolipoprotein E gene.

Vertex-wise and lobar ODI results were visualized using Surfice (<https://www.nitrc.org/plugins/mwiki/index.php/surface:MainPage>) and the R package GGSEG, respectively.

Results

Sample characteristics

Participant characteristics are summarized in Table 1. Across the total sample (N = 1954), there were 1197 non-carriers [ε2/ε2: N = 5 (0.3%), ε2/ε3: N = 133 (6.8%), ε3/ε3: N = 1059 (54.2%)], and 757 APOE ε4 carriers [ε2/ε4: N = 43 (2.2%), ε3/ε4: N = 616 (31.5%) and ε4/ε4: N = 98 (5%)]. The mean (SD) age of the sample was 57 ± 7.3, ranging from 40 to 77.1. There were no significant differences in age (P = 0.73), sex distribution (P = 0.44) and years of

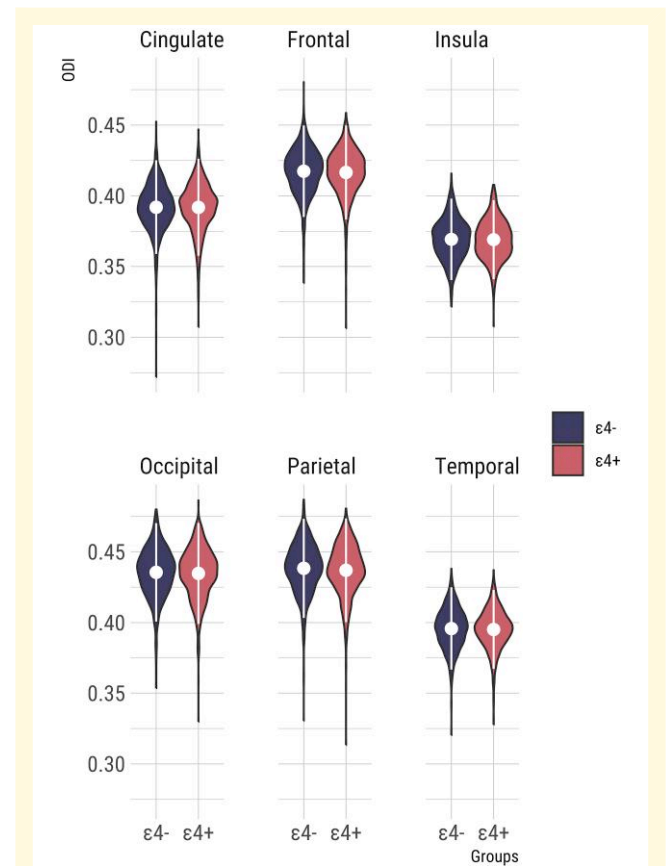


Figure 1 Violin plots of mean lobar ODI in APOE ε4 carriers and non-carriers. Non-parametric permutation tests of group differences using PALM revealed no significant differences between both groups after adjusting for multiple comparisons with FWE (frontal: $T = 1.5$, $P_{FWE} = 0.82$, parietal: $T = 2.2$, $P_{FWE} = 0.75$, temporal: $T = 0.9$, $P_{FWE} = 0.88$, occipital: $T = 1.1$, $P_{FWE} = 0.86$, cingulate: $T = 0.2$, $P_{FWE} = 0.98$, insula: $T = 0.4$, $P_{FWE} = 0.94$). Abbreviations: APOE, Apolipoprotein E gene; FWE, family wise error; ODI, Orientation Dispersion Index; PALM, Permutation Analysis of Linear Models.

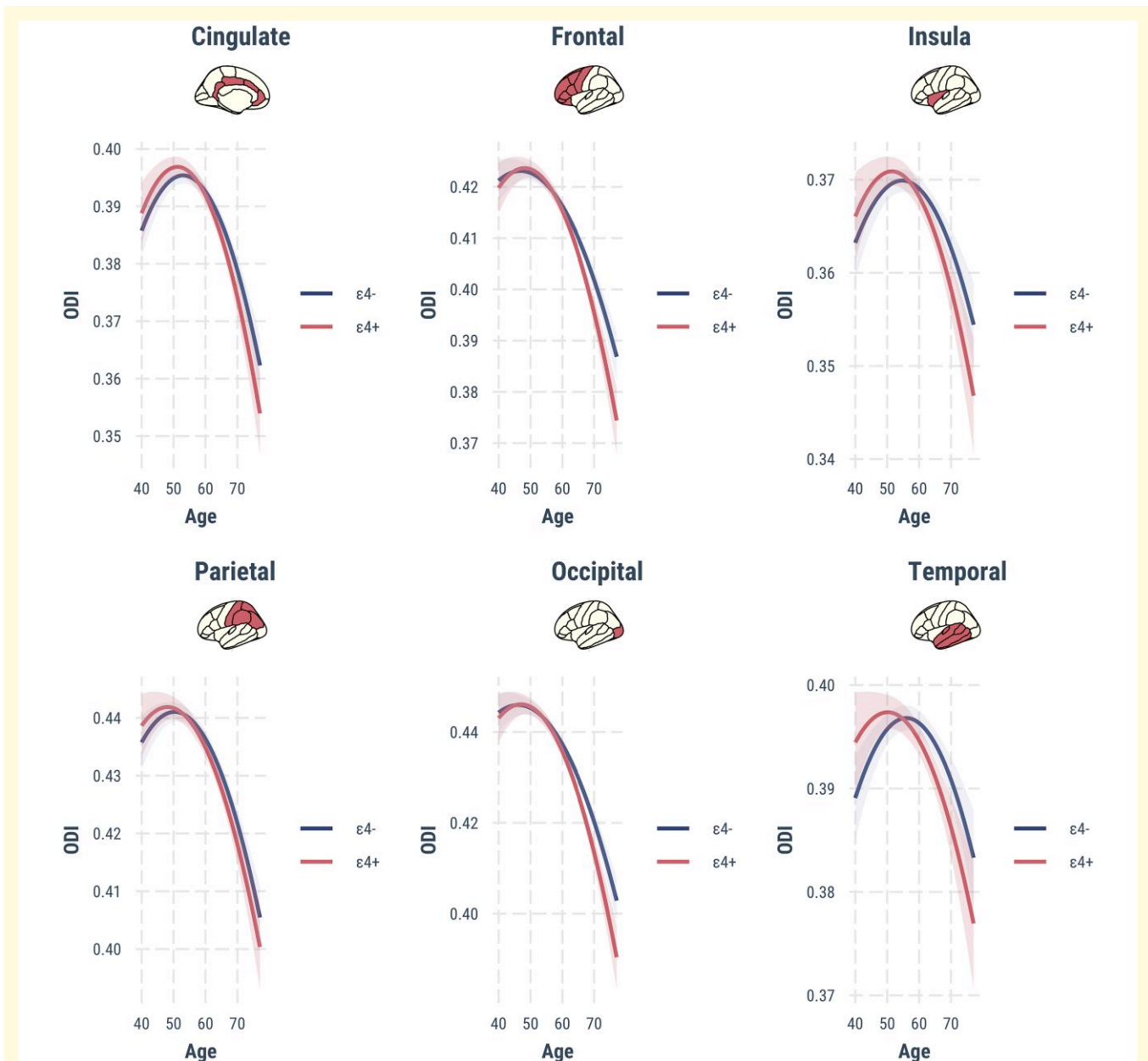


Figure 2 Marginal effect graphs depicting the two-way interactions between *APOE* $\epsilon 4$ and age (x-axis) on lobar ODI values (y-axis). Individuals with the *APOE* $\epsilon 4$ allele showed significantly steeper age-related reductions in ODI compared with non-carriers in the cingulate, frontal, insula, parietal and temporal lobes. Statistical significance was determined in PALM using non-parametric permutation models (5000 permutations, $P_{FWE} < 0.05$, adjusted for gender, years of formal education and sites). *APOE*, Apolipoprotein E gene; FWE, family wise error; ODI, Orientation Dispersion Index; PALM, Permutation Analysis of Linear Models.

education ($P = 0.23$) between the *APOE* $\epsilon 4$ carriers and non-carriers.

Main effects of *APOE* $\epsilon 4$

Violin plots of lobar ODI in *APOE* $\epsilon 4$ carriers and non-carriers are shown in Fig. 1. Both groups did not differ in terms of lobar ODI (frontal: $T = 1.5$, $P_{FWE} = 0.82$, parietal: $T = 2.2$, $P_{FWE} = 0.75$, temporal: $T = 0.9$, $P_{FWE} = 0.88$, occipital: $T = 1.1$, $P_{FWE} = 0.86$, cingulate: $T = 0.2$, $P_{FWE} =$

0.98 , insula: $T = 0.4$, $P_{FWE} = 0.94$), and effect sizes were small (Cohen's D : 0.01–0.13). Similarly, vertex-wise analyses revealed no significant clusters of ODI differences between the two groups (threshold free cluster enhancement with FWE rate adjustment; TFCE $P_{FWE} > 0.05$).

APOE $\epsilon 4 \times$ age

There were significant *APOE* $\epsilon 4 \times$ age interactions in the frontal, parietal, temporal, cingulate and insula lobes,

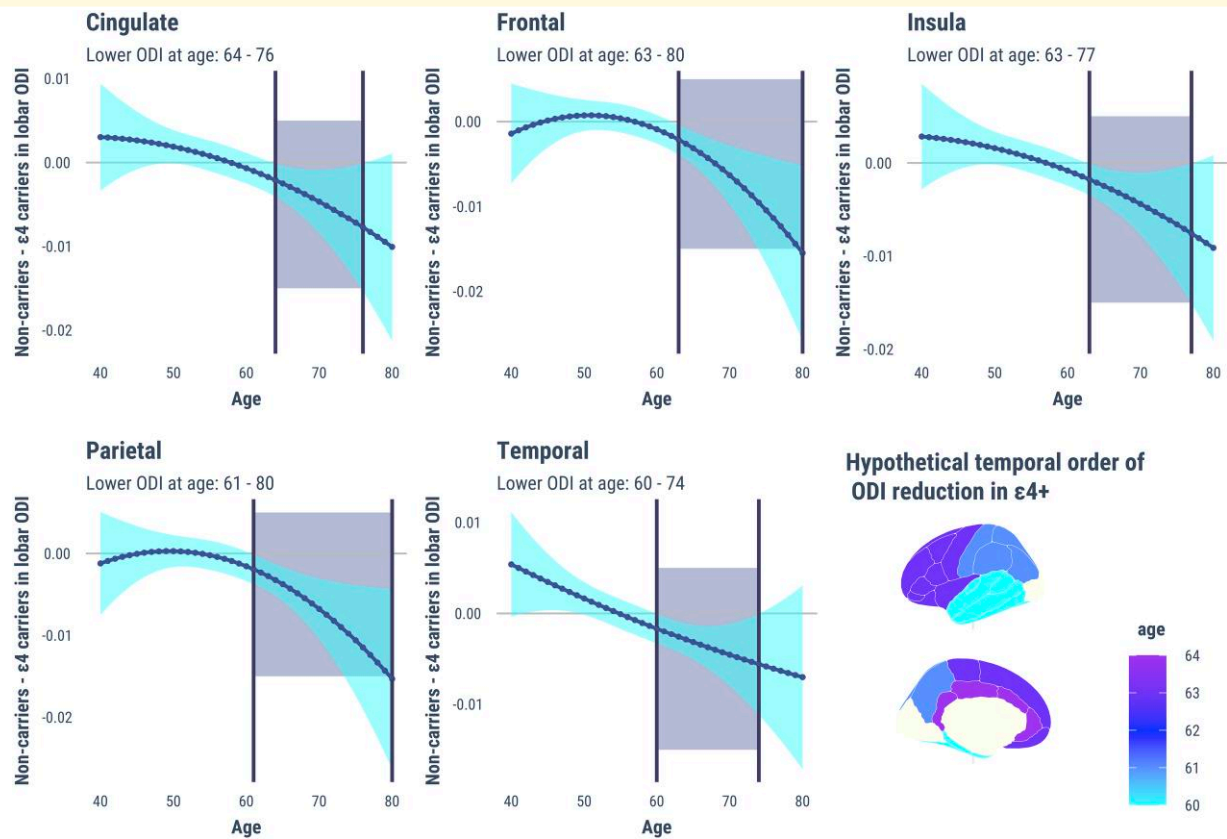


Figure 3 Differences in standardized lobar ODI between *APOE* $\epsilon 4$ carriers and non-carriers (y-axis) as a function of age (x-axis). Pairwise comparisons were calculated based on marginal effects to predict the earliest hypothetical age at which *APOE* $\epsilon 4$ carriers would show decreased lobar ODI relative to non-carriers, highlighted by the vertical dotted lines on the x-axis. The shaded cyan region represents the 95% confidence interval. For each lobe, the earliest age of significant ODI reductions in *APOE* $\epsilon 4$ carriers is illustrated in the choropleth brain map. Abbreviations: *APOE*, Apolipoprotein E gene; ODI, Orientation Dispersion Index.

indicating differential age-dependent ODI reductions in *APOE* $\epsilon 4$ carriers relative to non-carriers (frontal: $T = 2.7$, parietal: $T = 2.7$, temporal: $T = 3.6$, cingulate: $T = 2.1$, insula: $T = 3$, $P_{FWE} < 0.05$).

Plots of marginal effects showed steeper age-related decreases in ODI for *APOE* $\epsilon 4$ carriers compared with non-carriers (Fig. 2). To estimate the hypothetical inflection points of divergent ODI age trends, we calculated between-group differences of the predicted ODI from age 40 to 80 and determined the earliest age at which the differences emerged (Fig. 3). In general, lobar ODIs were similar between *APOE* $\epsilon 4$ carriers and non-carriers from age 40 to 60, after which significant reductions in ODI became more apparent in *APOE* $\epsilon 4$ compared with the non-carriers (temporal: age = 60–74, cingulate: age = 64–76, frontal: age = 63–80, insula: age = 63–77 and parietal: age = 61–80).

Next, we used an unbiased vertex-wise approach to map the topography of the *APOE* $\epsilon 4$ age interactions across the cortex. Significant clusters were found primarily in the temporo-parietal cortices and the frontal lobe (Fig. 4). Figure 5 tabulates the summary statistics and MNI coordinates of the peak effects in each cluster. There were no

significant interactions between *APOE* $\epsilon 4$ and age on lobar cortical thickness ($P_{FWE} > 0.05$).

APOE $\epsilon 4$ \times age \times education interactions

Three-way interactions of *APOE* $\epsilon 4$ \times age \times education were found in the frontal, parietal lobes ($P_{FWE} < 0.05$), indicating steeper age-related reductions in ODI among *APOE* $\epsilon 4$ carriers with lower years of education (mean -1 SD). *Post hoc* stratified analyses in *APOE* $\epsilon 4$ carriers and non-carriers confirmed that the age \times education interaction was significant only among *APOE* $\epsilon 4$ carriers [frontal: $T = 2.68$, parietal $T = 2.37$ and $P_{FWE} < 0.05$ (Fig. 6)].

The fronto-parietal lobar patterns of *APOE* $\epsilon 4$ \times age \times education interactions were corroborated by vertex-wise permutation analyses, which revealed peak effects in the rostral left middle frontal and precentral gyri (Fig. 7; TFCE $P_{FWE} < 0.05$). The summary statistics and MNI coordinates of the peak effects in each cluster are shown in Fig. 8. There were no significant three-way interactions between *APOE* $\epsilon 4$ \times age \times education on lobar cortical thickness.

Sensitivity analyses

A series of sensitivity analyses were performed to determine the robustness of our key findings against potential confounds. (i) All analyses were repeated after excluding the *APOE* $\epsilon 2\epsilon 4$ carriers due to the genetic ambiguity of

contrasting risk profiles. (ii) To investigate whether the *APOE* $\epsilon 4$ effects on ODI are independent of atrophy, we additionally adjusted for mean cortical thickness. All the findings were unchanged. Detailed results for these analyses are provided in the [Supplementary Materials](#).

Discussion

Our findings demonstrate more pronounced age-related declines in cortical ODI among *APOE* $\epsilon 4$ carriers compared with non-carriers. The interactions of *APOE* $\epsilon 4$ and age were most prominent in the temporo-parietal lobes, which are known to be more vulnerable to early neurodegeneration and accumulation of Alzheimer's disease abnormalities. Second, our analyses of the three-way interactions between *APOE* $\epsilon 4$, age, and education showed that the detrimental effects of *APOE* $\epsilon 4$ with increased age were most strongly expressed in $\epsilon 4$ carriers with lower levels of education, suggesting that high levels of cognitive reserve could mitigate against the accelerated ODI decline in $\epsilon 4$ carriers. Finally, these findings were independent of cortical atrophy. While conclusions are limited due to the cross-sectional design, our findings imply that *APOE* $\epsilon 4$ -related changes in ODI may precede macroscopically visible changes in cortical atrophy and may be a more sensitive marker of incipient Alzheimer's disease.

A growing body of evidence suggests that *APOE* $\epsilon 4$ is a potent moderator of age-related trends for imaging biomarkers.^{17,19,48,49} Indeed, we observed widespread interactions between age and *APOE* $\epsilon 4$ on ODI, characterized by steeper age-dependent ODI reductions in *APOE* $\epsilon 4$ carriers compared with non-carriers. Insofar as ODI is a valid proxy

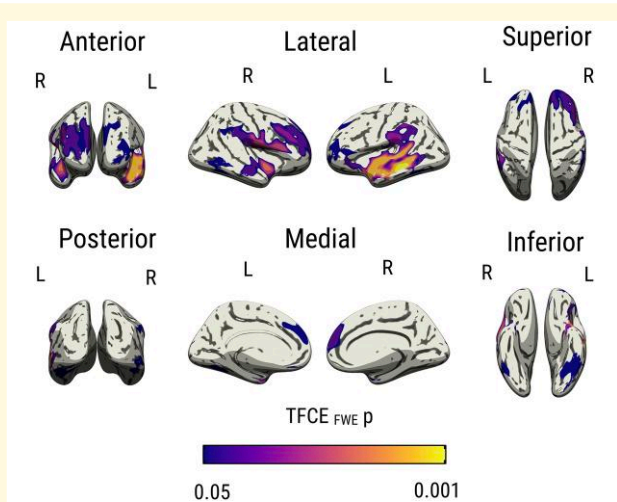


Figure 4 Vertex-wise interactions between *APOE* $\epsilon 4$ and age on cortical ODI. Results were obtained using non-parametric permutation models, implemented using PALM on ComBat harmonized ODI surface maps, and significance was established with TFCE $P_{FWE} < 0.05$, adjusted for sex, years of formal education and site. Abbreviations: *APOE*, Apolipoprotein E gene; TFCE, Threshold Free Cluster Enhancement; FWE, Family Wise Error; ODI, Orientation Dispersion Index; PALM, Permutation Analysis of Linear Models.

Cluster	Regions	Max T	X	Y	Z
	L middle temporal	2.97	-62.20	-34.90	-9.50
	L superior frontal	1.41	-6.70	47.40	36.60
	L medial orbitofrontal	1.32	-4.90	39.20	-18.90
	R postcentral	2.30	57.00	-7.70	10.80
	R superior temporal	2.31	41.50	-10.80	-11.80
	R middle temporal	1.43	53.20	-49.90	-1.40
	R entorhinal	1.32	26.10	-3.80	-25.60

Figure 5 Summary statistics and MNI152 coordinates significant cluster associated with the *APOE* $\epsilon 4 \times$ age interaction on vertex-wise ODI (TFCE $P_{FWE} < 0.05$, adjusted for sex, years of formal education, and site). Abbreviations: *APOE*, Apolipoprotein E gene; TFCE, Threshold Free Cluster Enhancement; FWE, family wise error; ODI, Orientation Dispersion Index; MNI152, Montreal Neurological Institute 152.

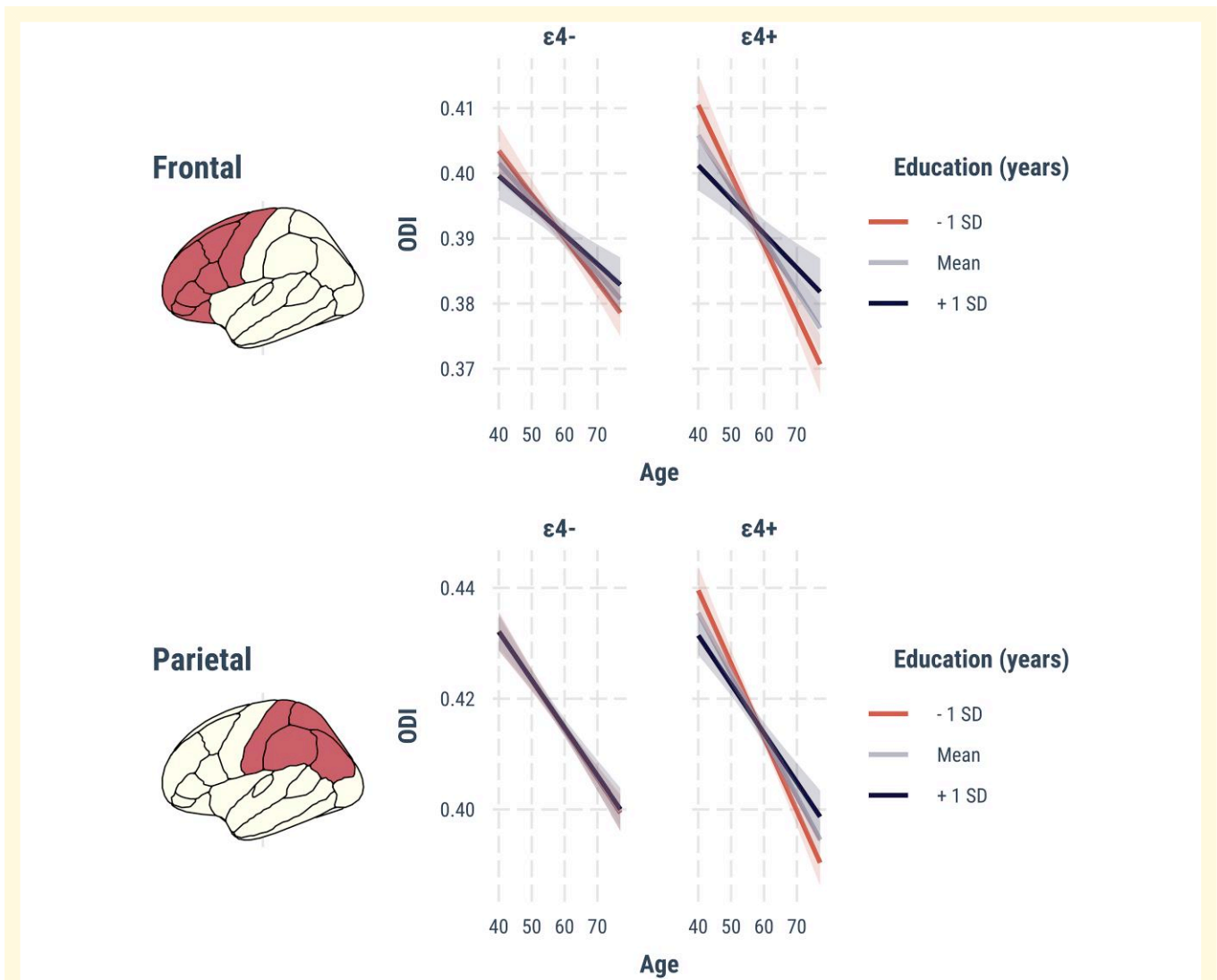


Figure 6 Three-way interactions between APOE $\epsilon 4$ \times age \times education. Marginal effects are depicted for the frontal and parietal lobes, stratified by APOE $\epsilon 4$ status. Lower years of education (mean–1 SD) are associated with steeper age-dependent reductions of ODI among the $\epsilon 4$ carriers only (frontal: $T = 2.68$, parietal: $T = 2.37$, $P_{FWE} < 0.05$, adjusted for site and sex). Abbreviations: APOE, Apolipoprotein E gene; FWE, family wise error; SD, standard deviation; ODI, Orientation Dispersion Index.

for dendritic complexity,^{28,29} our findings could also be interpreted as an *in vivo* extension of a previous histological study in which Alzheimer's disease APOE $\epsilon 4$ carriers exhibited a marked loss of dendritic outgrowth and synaptic count relative to non-carriers.⁵⁰ Loss of dendritic arborization is a common phenomenon associated with the ageing brain,⁵¹ and previous NODDI studies have demonstrated age-related decline with ODI.^{30,52} The main novel aspect of our finding, however, is that the presence APOE $\epsilon 4$ allele may further exacerbate the age-dependent decline in ODI. The interactions between APOE $\epsilon 4$ and age are also broadly consistent with data from other imaging modalities, including accelerated grey matter atrophy,⁵³ alterations in myelination,¹⁷ hippocampal shape,^{18,19} glucose metabolism⁵⁴ and cerebral perfusion.^{10,55} More broadly, these studies suggest that the previously outlined inconsistencies in the literature could

be clarified by taking into account the non-uniform effects of APOE4 across age in the future.

Marginal effect analyses revealed that cortical ODI trajectories diverged between APOE 4 allele carriers and non-carriers around the age of 60 (i.e. temporal lobe). While additional longitudinal studies are required to validate these results, our data may hint at the existence of an inflection point (age = 60) prior to the appearance of more severe grey matter deficits in APOE $\epsilon 4$ carriers. Multiple lines of research seem to support this notion. For instance, it has been shown that APOE $\epsilon 4$ is more closely associated with Alzheimer's disease neuropathology after the age of 60.⁵⁶ Within the context of current biomarker models in Alzheimer's disease,⁵⁷ our results positioned the onset of APOE $\epsilon 4$ -related ODI alterations (age = 60) in close temporal proximity with the exponential build-up of amyloid

(age = 60),⁵⁸ roughly a decade before the onset of cognitive impairment *APOE* $\epsilon 4$ (age = 69).^{59,60} These studies, including our own findings, lend support to the hypothesis that the detrimental consequences of *APOE* $\epsilon 4$ are more pronounced after the sixth decade.

Although the molecular pathways by which age and *APOE* $\epsilon 4$ interact to influence cortical microstructure remain poorly understood, several lines of research support the biological plausibility of our findings. (i) First, *APOE* $\epsilon 4$ may influence age-related ODI declines via tau-related pathways.^{58,61} Recent evidence suggests that cognitively normal *APOE* $\epsilon 4$ carriers accumulate tau and amyloid at a quicker rate beginning at age 60, which coincides with our findings in the temporal lobe ODI (earliest divergence between *APOE* $\epsilon 4$ and non-carriers at age 60).⁵⁸ Indeed, our vertex-wise analyses demonstrated that the most prominent effects were localized within the temporal cortices (e.g.

entorhinal cortex, inferior temporal cortex)—early predilection sites for neurofibrillary tangles.⁶² Previous data from transgenic mice⁶³ and neuropathological studies have also shown that *APOE* $\epsilon 4$ is related to increased tau deposition in the temporal cortex.⁶⁴ In addition, lower cortical ODI has been observed in rTg4510 transgenic mice model.⁶⁵ Our group has recently demonstrated *in vivo* reductions of ODI in patients with primary tauopathies,³² and lower ODI has been correlated with increased uptake of the PET [18F] THK5351 tracer in an Alzheimer's disease sample.⁶⁶ (ii) Second, amyloid deposition may also play a role, since 10–15% of *APOE* $\epsilon 4$ participants in our cohorts are anticipated to have elevated amyloid burden.^{67,68} It has been shown that dendritic branching in close proximity to amyloid deposits exhibits bending abnormalities, more abrupt branch terminations and spine loss.⁶⁹ Future research integrating multi-modal imaging with CSF or plasma biomarkers⁷⁰ would be well-suited to distinguish the unique contributions of Alzheimer's disease pathologies to changes in cortical ODI. In order to establish whether our vertex-wise findings reflect the 'penumbra' of subsequent atrophy, longitudinal studies comprising a wider spectrum of cognitively normal *APOE* $\epsilon 4$ carriers, individuals with MCI and Alzheimer's disease are warranted.

A secondary aim of this study was to determine the degree to which education may attenuate the adverse effects of *APOE* $\epsilon 4$ on age-related ODI changes. To that end, our lobar and vertex-wise analyses indicated a significant three-way interaction between age, *APOE* $\epsilon 4$ and education years in the fronto-parietal cortices; i.e. steeper age-dependent ODI reductions were observed in *APOE* $\epsilon 4$ carriers with less education. In contrast, the impact of *APOE* $\epsilon 4$ on age-related ODI changes in individuals with more years of education was negligible. As such, our findings lend support to previous findings indicating that more years of education was a significant predictor of less cognitive change over time among *ApoE* $\epsilon 4$ carriers⁷¹ and are aligned with post-mortem evidence, suggesting that higher education may mitigate the deleterious effects of senile plaques⁷² The involvement of fronto-parietal cortices may also be interpreted in light of their roles as key neural substrates of working memory.⁷³ Indeed, a recent study has shown that education beyond high school may mitigate the effects of *APOE* $\epsilon 4$ on working

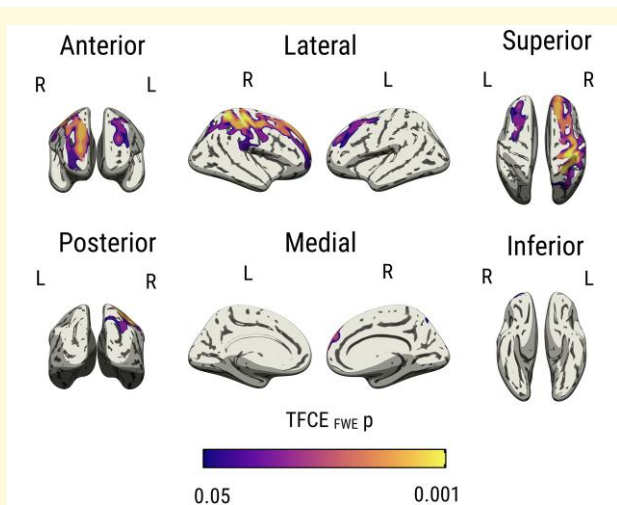


Figure 7 Vertex-wise three-way interactions between *APOE* $\epsilon 4$ × age × education. Marginal effects are depicted for the frontal and parietal lobes, stratified by *APOE* $\epsilon 4$ status. Lower years of education (mean–1 SD) are associated with steeper age-dependent reductions of ODI among the $\epsilon 4$ carriers only ($P_{FWE} < 0.05$, adjusted for site and sex). Abbreviations: *APOE*, Apolipoprotein E gene; FWE, family wise error; SD, standard deviation; ODI, Orientation Dispersion Index.

Cluster	Regions	Max T	X	Y	Z
	L rostral middle frontal	2.06	-24.30	36.30	25.00
	R precentral	2.82	30.10	-23.50	44.50

Figure 8 Summary statistics and MNI 152 coordinates for each significant cluster associated with the three-way interactions of *APOE* $\epsilon 4$ × age × education interaction on vertex-wise ODI. Abbreviations: *APOE*, Apolipoprotein E gene; ODI, Orientation Dispersion Index; MNI 152, Montreal Neurological Institute 152.

memory.¹⁵ Collectively, these findings support a scenario in which a diminished ‘cognitive reserve’ may lead to greater age-related susceptibility to the *APOE* ε4 allele.¹⁶

Notably, our ODI findings persisted after controlling for cortical thickness. Moreover, we did not find any significant effects of *APOE* ε4 carriership on cortical thickness (i.e. effects may only appear in *APOE* ε4 homozygotes at this age range). The null results of *APOE* ε4 on cortical thickness could be anticipated in light of the inconsistent findings and modest effect sizes in the literature. Grey matter atrophy is also thought to reflect downstream neurodegenerative changes occurring later in the course of Alzheimer’s disease.⁷⁴ Under the assumption that a cross-sectional estimate of a biomarker represents its accumulated pathological burden, the combination of ODI changes and the absence of cortical thickness effects is compatible with early loss of dendritic arborization before cell death and atrophy.^{75,76} Similarly, greater magnitudes of changes seen in NODDI relative to that of atrophy have been demonstrated in studies of people with primary tauopathies,³² young-onset Alzheimer’s disease,³⁴ MCI and Alzheimer’s disease.⁷⁷ Taken together, our findings suggest that NODDI may serve as a promising biomarker to reveal unique insights into subtle grey matter deficits in preclinical dementia.

There are several caveats to consider when interpreting our results. (i) Our cross-sectional design precludes definitive conclusions regarding the role of *APOE* ε4 in predicting age-related trends of ODI reduction. Therefore, conclusions of group differences at different ages should be considered preliminary. Prospective longitudinal studies are necessary to determine if the intra-individual rates of ODI reductions are (ii) significantly accelerated in *APOE* ε4 carriers and (iii) whether they are associated with cognitive decline. While our findings revealed robust associations between *APOE* ε4 and accelerated reductions in ODI, the pathological processes underpinning this relationship remain unclear. Additional investigations using fluid biomarkers or PET imaging would be required to characterize the pathogenic processes that may underlie the *APOE* ε4-related ODI alterations. Leveraging multi-modal data will facilitate analyses to investigate potential interactions of *APOE* ε4 with other pathological markers on ODI. The lack of amyloid status on our participants is another limitation, and future studies are needed to determine whether findings are consistent in amyloid-negative *APOE* ε4 carriers. (iv) The ODI parameters were determined from diffusion-weighted single-shell datasets as opposed to multi-shell NODDI sequences. Nonetheless, the feasibility of estimating ODI from single-shell DWI had been demonstrated in the seminal NODDI study,²⁷ and subsequent groups have confirmed that ODI maps calculated using multi-shell and single-shell ($b = 1000 \text{ s/mm}^2$) are highly comparable and exhibit a high degree of overlap with respect to group differences.⁴³ (v) While we have interpreted ODI reductions as suggestive of dendritic arborization loss, histological validation of NODDI measurements remains confined to post-mortem spinal cord specimens from patients with multiple

sceleroides.²⁹ More research triangulating data from *ex vivo* imaging, post-mortem samples and PET imaging would be required to draw firmer conclusions on the specific cellular abnormalities revealed by ODI. (vi) Lower education years increased the detrimental effect of *APOE* ε4 on age-related ODI declines; however, interpretations should also account for the extensive relationships of education with general health, environmental enrichment and socio-economic status, all of which could significantly moderate the associations between education and *APOE* ε4-related ODI decreases. (vii) Another limitation of the current study is our exclusive focus on older adults with normal cognitive function. By restricting our sample to non-impaired individuals, we aimed to delineate structural brain changes associated with *APOE* ε4 in the preclinical stage, prior to the onset of overt symptoms. Therefore, our findings may not generalize to later stages of dementia, where relationships between *APOE* ε4 status and brain structure may be more complex.

In summary, we have conducted a comprehensive analysis of *APOE* ε4 carriership and its impact on age-related patterns of ODI alterations in one of the largest datasets of cognitively normal persons in midlife. We found novel evidence that *APOE* ε4 worsened age-related ODI decreases in brain regions typically associated with atrophy patterns of Alzheimer’s disease. This finding also suggests that *APOE* ε4 may hasten the onset age of dementia by accelerating age-dependent reductions in cortical ODI, although additional studies are needed to verify this hypothesis. Finally, our research lends methodological support to the use of NODDI as a sensitive surrogate for changes in grey matter microstructure.

Supplementary material

Supplementary material is available at *Brain Communications* online.

Acknowledgements

We would like to thank our participant volunteers for taking part in this study. We are also appreciative of the computational infrastructure that enabled data analysis and storage; this was made possible by the High Performance Hubs for Clinical Informatics (HPHI), which was sponsored by the MRC Research Infrastructure Award (MR/M009041/1).

Funding

The research leading to these results has received funding from ‘la Caixa’ Foundation. Additional funding was obtained from Fondo de Investigacion Sanitaria (FIS), ‘la Caixa’ Foundation under grant PI12/00326. J.D.G. holds a ‘Ramon y Cajal’ fellowship (RYC-2013-13054). This work was funded by a grant for the PREVENT-Dementia program from the United Kingdom Alzheimer’s Society (grant numbers 178 and 264),

the United States Alzheimer's Association (grant number TriBEKa-17-519007) and philanthropic donations. L.S. is supported by the Cambridge National Institute for Health and Care Research, Biomedical Research Center, and Alzheimer's Research UK (ARUK-SRF2017B-1). J.T.O.B. receives infrastructural support from the Cambridge National Institute for Health and Care Research, Biomedical Research Center. E.M. is supported by an Alzheimer's Society Junior Research Fellowship (443 AS JF 18017).

Competing interests

Unrelated to this work, J.T.O.B. has received honoraria for work as DSMB chair or member for TauRx, Axon, Eisai, has acted as a consultant for Roche, and has received research support from Alliance Medical and Merck.

Data availability

The data supporting the conclusions described in this paper are available upon reasonable request from the corresponding author.

Appendix

Members of the PREVENT Dementia group

Katie Bridgeman, Leonidas Chouliaras, Siobhan Coleman, Hannah Darwin, David Driscoll, Maria-Elena Dounavi, Robert Dudas, Sarah Gregory, Ivan Koychev, Brian Lawlor, Audrey Low, Elijah Mak, Clare Mackay, Paresh Malhotra, Jean Manson, Graciela Muniz-Terrera, Lorina Naci, T. John O'Brien, Richard Oakley, Vanessa Raymont, Craig Ritchie, Karen Ritchie, William Stewart, Li Su, Peter Swann, Tony Thayanandan, B. Guy Williams.

Members of the ALFA study group

Ricardo A. Aguilar, Annabella B. Gorriti, Anna B. Serrat, Raffaele Cacciaglia, Lidia C. Gispert, Alba C. Martinez, Marta D. Milan, Carmen D. Gomez, Ruth D. Iglesias, Marie E. F. Karine, Sherezade F. Julian, Patricia G. Serra, Juan D. Gispert, Armand G. Escalante, Oriol G. Rivera, Laura H. Penas, Gema H. Rodriguez, Jordi H. Ninou, Laura I. Gamez, Iva Knezevic, Paula M. Alvarez, Tania M. Diaz, Carolina M. Gil, Eva Palacios, Maria Pascual, Albina P. Ballester, Sandra P. Mendez, Irina A. Radoi, Blanca R. Fernandez, Laura R. Freixedes, Aleix S. Vila, Gonzalo A. Sanchez Benavides, Mahnaz S. Mahnaz, Lluís S. Harster, Anna S. Prat, Laura S. Stankeviciute, Marc S. Calvet, Marc V. Jaramillo, Natalia V. Tejedor.

References

1. Corder EH, Saunders AM, Strittmatter WJ, et al. Gene dose of apolipoprotein E type 4 allele and the risk of Alzheimer's disease in late onset families. *Science*. 1993;261(5123):921-923.
2. Strittmatter WJ, Roses AD. Apolipoprotein E and Alzheimer's disease. *Annu Rev Neurosci*. 1996;19:53-77.
3. Habib M, Mak E, Gabel S, et al. Functional neuroimaging findings in healthy middle-aged adults at risk of Alzheimer's disease. *Ageing Res Rev*. 2017;36:88-104.
4. Mak E, Gabel S, Mirette H, et al. Structural neuroimaging in preclinical dementia: From microstructural deficits and grey matter atrophy to macroscale connectomic changes. *Ageing Res Rev*. 2017;35:250-264.
5. Dounavi ME, Mak E, Wells K, et al. Volumetric alterations in the hippocampal subfields of subjects at increased risk of dementia. *Neurobiol Aging*. 2020;91:36-44.
6. Pievani M, Rasser P, Galluzzi S, et al. Mapping the effect of APOE ε4 on gray matter loss in Alzheimer's disease *in vivo*. *Neuroimage*. 2009;45(4):1090-1098.
7. ten Kate M, Barkhof F, Visser PJ, et al. Amyloid-independent atrophy patterns predict time to progression to dementia in mild cognitive impairment. *Alzheimers Res Ther*. 2017;9(1):73.
8. Adluru N, Destiche DJ, Lu SYF, et al. White matter microstructure in late middle-age: Effects of apolipoprotein E4 and parental family history of Alzheimer's disease. *Neuroimage Clin*. 2014;4:730-742.
9. Chen K, Ayutyanont N, Langbaum JBS, et al. Correlations between FDG PET glucose uptake-MRI gray matter volume scores and apolipoprotein e ε4 gene dose in cognitively normal adults: A cross-validation study using voxel-based multi-modal partial least squares. *Neuroimage*. 2012;60(4):2316-2322.
10. Mosconi L, Sorbi S, Nacmias B, et al. Age and ApoE genotype interaction in Alzheimer's disease: An FDG-PET study. *Psychiatry Res*. 2004;130(2):141-151.
11. Reiman EM, Caselli RJ, Yun LS, et al. Preclinical evidence of Alzheimer's disease in persons homozygous for the ε4 allele for apolipoprotein E. *N Engl J Med*. 1996;334(12):752-758.
12. Trachtenberg AJ, Filippini N, Mackay CE. The effects of APOE-ε4 on the BOLD response. *Neurobiol Aging*. 2012;33(2):323-334.
13. Cacciaglia R, Operto G, Falcón C, et al. Genotypic effects of APOE-ε4 on resting-state connectivity in cognitively intact individuals support functional brain compensation. *Cereb Cortex*. 2023;33(6):2748-2760.
14. Sheline YI, Morris JC, Snyder AZ, et al. APOE4 allele disrupts resting state fMRI connectivity in the absence of amyloid plaques or decreased CSF Aβ42. *J Neurosci*. 2010;30(50):17035-17040.
15. Vonk MJ, Arce Rentería M, Medina VM, et al. Education moderates the relation between APOE ε4 and memory in nondemented non-hispanic black older adults. *J Alzheimers Dis*. 2019;72(2):495-506.
16. Arenaza-Urquijo EM, Gonneaud J, Fouquet M, et al. Interaction between years of education and APOEε4 status on frontal and temporal metabolism. *Neurology*. 2015;85(16):1392-1399.
17. Operto G, Molinuevo JL, Cacciaglia R, et al. Interactive effect of age and APOE-ε4 allele load on white matter myelin content in cognitively normal middle-aged subjects. *Neuroimage Clin*. 2019;24:101983.
18. Cacciaglia R, Molinuevo JL, Falcón C, et al. APOE-ε4 shapes the cerebral organization in cognitively intact individuals as reflected by structural gray matter networks. *Cereb Cortex*. 2020;30(7):4110-4120.
19. Martí-Juan G, Sanroma-Guell G, Cacciaglia R, et al. Nonlinear interaction between APOE ε4 allele load and age in the hippocampal surface of cognitively intact individuals. *Hum Brain Mapp*. 2021;42(1):47-64.

20. Dumanis SB, Tesoriero JA, Babus LW, *et al.* Apoe4 decreases spine density and dendritic complexity in cortical neurons *in vivo*. *J Neurosci.* 2009;29(48):15317-15322.
21. Crombe A, Planche V, Raffard G, *et al.* Deciphering the microstructure of hippocampal subfields with *in vivo* DTI and NODDI: Applications to experimental multiple sclerosis. *Neuroimage.* 2018;172:357-368.
22. Montal V, Vilaplana E, Pegueroles J, *et al.* Biphasic cortical macro- and microstructural changes in autosomal dominant Alzheimer's disease. *Alzheimers Dement.* 2020;17(4):618-628.
23. Seitz J, Rathi Y, Lyall A, *et al.* Alteration of gray matter microstructure in schizophrenia. *Brain Imaging Behav.* 2018; 12(1):54-63.
24. Weston PSJ, Simpson IJA, Ryan NS, Ourselin S, Fox NC. Diffusion imaging changes in grey matter in Alzheimer's disease: A potential marker of early neurodegeneration. *Alzheimers Res Ther.* 2015; 7(1):47.
25. Torso M, Bozzali M, Zamboni G, Jenkinson M, Chance SA. Detection of Alzheimer's disease using cortical diffusion tensor imaging. *Hum Brain Mapp.* 2020;42(4):967-977.
26. Henf J, Grothe MJ, Brueggen K, Teipel S, Dyrba M. Mean diffusivity in cortical gray matter in Alzheimer's disease: The importance of partial volume correction. *Neuroimage Clin.* 2017;17: 579-586.
27. Zhang H, Schneider T, Wheeler-Kingshott CA, Alexander DC. NODDI: Practical *in vivo* neurite orientation dispersion and density imaging of the human brain. *Neuroimage.* 2012;61(4): 1000-1016.
28. Jespersen SN, Kroenke CD, Østergaard L, Ackerman JJH, Yablonskiy DA. Modeling dendrite density from magnetic resonance diffusion measurements. *Neuroimage.* 2007;34(4):1473-1486.
29. Grussu F, Schneider T, Tur C, *et al.* Neurite dispersion: A new marker of multiple sclerosis spinal cord pathology? *Ann Clin Transl Neurol.* 2017;4(9):663-679.
30. Nazeri A, Chakravarty MM, Rotenberg DJ, *et al.* Functional consequences of neurite orientation dispersion and density in humans across the adult lifespan. *J Neurosci.* 2015;35(4):1753-1762.
31. Venkatesh A, Stark SM, Stark CEL, Bennett IJ. Age- and memory-related differences in hippocampal gray matter integrity are better captured by NODDI compared to single-tensor diffusion imaging. *Neurobiol Aging.* 2020;96:12-21.
32. Mak E, Holland N, Jones PS, *et al.* *In vivo* coupling of dendritic complexity with presynaptic density in primary tauopathies. *Neurobiol Aging.* 2021;101:187-198.
33. Jack CR, Knopman DS, Jagust WJ, *et al.* Hypothetical model of dynamic biomarkers of the Alzheimer's pathological cascade. *Lancet Neurol.* 2010;9(1):119-128.
34. Parker TD, Slattery CF, Zhang J, *et al.* Cortical microstructure in young onset Alzheimer's disease using neurite orientation dispersion and density imaging. *Hum Brain Mapp.* 2018;39(7): 3005-3017.
35. Ritchie CW, Ritchie K. The PREVENT study: A prospective cohort study to identify mid-life biomarkers of late-onset Alzheimer's disease. *BMJ Open.* 2012;2(6):e001893.
36. Molinuevo JL, Gramunt N, Gispert JD, *et al.* The ALFA project: A research platform to identify early pathophysiological features of Alzheimer's disease. *Alzheimers Dement.* 2016;2(2):82-92.
37. Avants BB, Tustison NJ, Song G, Cook PA, Klein A, Gee JC. A reproducible evaluation of ANTs similarity metric performance in brain image registration. *Neuroimage.* 2011;54(3):2033-2044.
38. Fischl B. FreeSurfer. *Neuroimage.* 2012;62(2):774-781.
39. Veraart J, Fieremans E, Novikov DS. Diffusion MRI noise mapping using random matrix theory. *Magn Reson Med.* 2015;76(5): 1582-1593.
40. Andersson JLR, Graham MS, Zsoldos E, Sotiropoulos SN. Incorporating outlier detection and replacement into a non-parametric framework for movement and distortion correction of diffusion MR images. *Neuroimage.* 2016;141:556-572.
41. Leemans A, Jones DK. The B-matrix must be rotated when correcting for subject motion in DTI data. *Magn Reson Med.* 2009;61(6):1336-1349.
42. Harms RL, Fritz FJ, Tobisch A, Goebel R, Roebroeck A. Robust and fast nonlinear optimization of diffusion MRI microstructure models. *Neuroimage.* 2017;155:82-96.
43. Timmers I, Roebroeck A, Bastiani M, Jansma B, Rubio-Gozalbo E, Zhang H. Assessing microstructural substrates of white matter abnormalities: A comparative study using DTI and NODDI. *PLoS One.* 2016;11(12):e0167884.
44. Greve DN, Fischl B. Accurate and robust brain image alignment using boundary-based registration. *Neuroimage.* 2009;48(1):63-72.
45. Fischl B, Dale AM. Measuring the thickness of the human cerebral cortex from magnetic resonance images. *Proc Natl Acad Sci U S A.* 2000;97(20):11050-11055.
46. Desikan RS, Ségonne F, Fischl B, *et al.* An automated labeling system for subdividing the human cerebral cortex on MRI scans into gyral based regions of interest. *Neuroimage.* 2006;31(3):968-980.
47. Fortin JP, Parker D, Tunç B, *et al.* Harmonization of multi-site diffusion tensor imaging data. *Neuroimage.* 2017;161:149-170.
48. Bartzokis G, Lu PH, Geschwind DH, Edwards N, Mintz J, Cummings JL. Apolipoprotein E genotype and age-related myelin breakdown in healthy individuals: Implications for cognitive decline and dementia. *Arch Gen Psychiatry.* 2006;63(1):63-72.
49. Cacciaglia R, Molinuevo JL, Falcón C, *et al.* Effects of APOE- ϵ 4 allele load on brain morphology in a cohort of middle-aged healthy individuals with enriched genetic risk for Alzheimer's disease. *Alzheimers Dement.* 2018;14(7):902-912.
50. Arendt T, Schindler C, Brückner MK, *et al.* Plastic neuronal remodeling is impaired in patients with Alzheimer's disease carrying apolipoprotein epsilon 4 allele. *J Neurosci.* 1997;17(2):516-529.
51. Duan H, Wearne SL, Rocher AB, Macedo A, Morrison JH, Hof PR. Age-related dendritic and spine changes in corticocortically projecting neurons in macaque monkeys. *Cereb Cortex.* 2003;13(9):950-961.
52. Mole JP, Fasano F, Evans J, *et al.* APOE- ϵ 4-related differences in left thalamic microstructure in cognitively healthy adults. *Sci Rep.* 2020;10(1):19787.
53. Espeseth T, Westlye LT, Fjell AM, Walhovd KB, Rootwelt H, Reinvang I. Accelerated age-related cortical thinning in healthy carriers of apolipoprotein E epsilon 4. *Neurobiol Aging.* 2008;29(3):329-340.
54. Mosconi L, Herholz K, Prohovnik I, *et al.* Metabolic interaction between ApoE genotype and onset age in Alzheimer's disease: Implications for brain reserve. *J Neurol Neurosurg Psychiatry.* 2005;76(1):15-23.
55. Wierenga CE, Clark LR, Dev SI, *et al.* Interaction of age and APOE genotype on cerebral blood flow at rest. *J Alzheimers Dis.* 2013; 34(4):921-935.
56. Saddiki H, Fayosse A, Cognat E, *et al.* Age and the association between apolipoprotein E genotype and Alzheimer disease: A cerebrospinal fluid biomarker-based casecontrol study. *PLoS Med.* 2020; 17(8):e1003289.
57. Jack CR, Knopman DS, Jagust WJ, *et al.* Tracking pathophysiological processes in Alzheimer's disease: An updated hypothetical model of dynamic biomarkers. *Lancet Neurol.* 2013;12(2):207-216.
58. Koychev I, Vaci N, Bilgel M, *et al.* Prediction of rapid amyloid and phosphorylated-Tau accumulation in cognitively healthy individuals. *Alzheimers Dement.* 2020;12(1):e12019.
59. Rawle MJ, Davis D, Bendayan R, Wong A, Kuh D, Richards M. Apolipoprotein-E (ApoE) ϵ 4 and cognitive decline over the adult life course. *Transl Psychiatry.* 2018;8(1):1-8.
60. Christensen H, Batterham PJ, Mackinnon AJ, *et al.* The association of APOE genotype and cognitive decline in interaction with risk factors in a 65-69 year old community sample. *BMC Geriatr.* 2008;8:14.
61. Shi Y, Yamada K, Liddelov SA, *et al.* Apoe4 markedly exacerbates tau-mediated neurodegeneration in a mouse model of tauopathy. *Nature.* 2017;549(7673):523-527.
62. Braak H, Braak E. Neuropathological staging of Alzheimer-related changes. *Acta Neuropathol.* 1991;82(4):239-259.

63. Brecht WJ. Neuron-specific apolipoprotein E4 proteolysis is associated with increased Tau phosphorylation in brains of transgenic mice. *J Neurosci.* 2004;24(10):2527-2534.
64. Tiraboschi P, Hansen LA, Masliah E, Alford M, Thal LJ, Corey-Bloom J. Impact of APOE genotype on neuropathologic and neurochemical markers of Alzheimer disease. *Neurology.* 2004;62(11):1977-1983.
65. Colgan N, Siow B, O'Callaghan JM, et al. Application of neurite orientation dispersion and density imaging (NODDI) to a tau pathology model of Alzheimer's disease. *Neuroimage.* 2016;125:739-744.
66. Sone D, Shigemoto Y, Ogawa M, et al. Association between neurite metrics and tau/inflammatory pathology in Alzheimer's disease. *Alzheimers Dement.* 2020;12(1):e12125.
67. Jack CR, Wiste HJ, Weigand SD, et al. Age, sex, and APOE ϵ 4 effects on memory, brain structure, and β -amyloid across the adult life span. *JAMA Neurol.* 2015;72(5):511-519.
68. Jansen WJ, Ossenkoppele R, Tijms BM, et al. Association of cerebral amyloid- β aggregation with cognitive functioning in persons without dementia. *JAMA Psychiatry.* 2018;75(1):84-95.
69. Grutzendler J, Helmin K, Tsai J, Gan WB. Various dendritic abnormalities are associated with fibrillar amyloid deposits in Alzheimer's disease. *Ann N Y Acad Sci.* 2007;1097:30-39.
70. Zetterberg H, Schott JM. Blood biomarkers for Alzheimer's disease and related disorders. *Acta Neurol Scand.* 2022;146(1):51-55.
71. Kaup AR, Nettiksimmons J, Harris TB, et al. Cognitive resilience to apolipoprotein E ϵ 4. *JAMA Neurol.* 2015;72(3):340.
72. Bennett DA, Wilson RS, Schneider JA, et al. Education modifies the relation of AD pathology to level of cognitive function in older persons. *Neurology.* 2003;60(12):1909-1915.
73. Casey BJ, Cohen JD, Jezzard P, et al. Activation of prefrontal cortex in children during a nonspatial working memory task with functional MRI. *Neuroimage.* 1995;2(3):221-229.
74. Jack Clifford R, Holtzman David M. Biomarker modeling of Alzheimer's disease. *Neuron.* 2013;80(6):1347-1358.
75. Ertürk A, Wang Y, Sheng M. Local pruning of dendrites and spines by caspase-3-dependent and proteasome-limited mechanisms. *J Neurosci.* 2014;34(5):1672-1688.
76. López-Doménech G, Higgs NF, Vaccaro V, et al. Loss of dendritic complexity precedes neurodegeneration in a mouse model with disrupted mitochondrial distribution in mature dendrites. *Cell Rep.* 2016;17(2):317-327.
77. Vogt NM, Hunt JF, Adluru N, et al. Cortical microstructural alterations in mild cognitive impairment and Alzheimer's disease dementia. *Cereb Cortex.* 2020;30(5):2948-2960.